Available online at www.sciencedirect.com
SCIENCE DIRECT®
PERGAMON
Polyhedron 22 (2003) 1355–1366
POLYHEDRON
www.elsevier.com/locate/poly

Synthesis, X-ray structural characterization and solution studies of metal complexes containing the anti-inflammatory drugs meloxicam and tenoxicam

Sandra Defazio, Renzo Cini *

Department of Chemical and Biosystem Sciences and Tecnologies, University of Siena, Via A. Moro 2, I-53100 Siena, Italy

Received 21 November 2002; accepted 17 February 2003

Abstract

The reaction of tenoxicam (H_2ten, 4-hydroxy-2-methyl-*N*-2-pyridyl-2H-thieno[2,3-e]-1,2-thiazine-3-carboxamide-1,1-dioxide), with $M(CH_3COO)_2$ (M = Cd, Co, Zn; 2:1 molar ratio) in hot methanol produced the microcrystalline compounds: $Cd^{II}(Hten)_2\cdot 2CH_3OH$, **1**, $Co^{II}(Hten)_2CH_3OH3H_2O$, **2**, $Zn^{II}(Hten)_22CH_3OH$, **3**. Single crystals of *trans*,*trans*-$[Cd^{II}(Hten)_2(dmso)_2]$ **4** (dmso, dimethylsulfoxide) were obtained on cooling hot dmso solutions of **1**. *trans*-$[PtCl_2(\eta^2\text{-}C_2H_4)(H_2ten)]$, **5** and *trans*-$[PtCl_2(\eta^2\text{-}C_2H_4)(H_2mel)]\cdot 0.5C_6H_6$, $\mathbf{6}\cdot 0.5C_6H_6$ were obtained from the reaction of the Zeise's salt $(K[PtCl_3(\eta^2\text{-}C_2H_4)]\cdot H_2O)$ with tenoxicam and meloxicam (4-hydroxy-2-methyl-*N*-(5-methyl-2-thiazolyl)-2H-1,2-benzothiazine-3-carboxammide-1,1-dioxide), respectively (1:1 molar ratio) in ethanol solution and subsequent recrystallization from benzene. Microcrystalline $Fe^{II}(Hmel)_2\cdot 4H_2O\cdot 2CH_3OH$, **7**, was prepared by reacting $Fe(CH_3COO)_2$ with H_2mel in refluxing methanol at a 1:2 molar ratio, under an atmosphere of ultrapure nitrogen. The X-ray diffraction structure of **4** consists of pseudo-octahedral complex molecules in which the two chelating $Hten^-$ anions (trans to each other) occupy the equatorial positions through the *O*-amide (Cd–O(15), 2.214(2) Å) and the *N*-pyridyl (Cd–N(1′), 2.303(3) Å) atoms. The conformation is ZZZ around the C(3)–C(14), C(14)–N(16) and N(16)–C(2′) bonds. The coordination sphere is completed by two oxygen atoms from two dmso ligands at the apical positions. The sulfur atom from the thieno system as well as the SO_2 function are not involved in any interactions to the metal; they contribute to the crystal packing via S···H–C and O···H–C hydrogen bond type interactions. The structures of **5** and **6** are similar each other as regards the coordination mode and overall conformation of the ligands (H_2ten and H_2mel, respectively). The platinum center links the nitrogen atom from pyridyl and thiazolyl rings with Pt–N bond lengths 2.077(5) and 2.072(13) Å, respectively. The EZE conformation of the neutral ligand molecules facilitates the formation of O(17)–H···O(15) strong intramolecular hydrogen bonds. The (N(16))H···Pt intramolecular contact distances are 2.54(1) (**5**) and 2.93(1) Å (**6**), suggesting that an attractive interactions may exist for **5** on the basis of van der Waals radii for H and Pt. The ^{1}H NMR data for **1** in dmso-d_6 show a general shift towards higher fields for signals of $Hten^-$ ligand with respect to those of free H_2ten. On the contrary the signals for H_2ten and H_2mel relevant to **5** and **6** ($CDCl_3$) undergo significant low field shifts upon the coordination to the platinum center. It is worth note that the signal for the H(16) atom is moved downfield by 1.93 ppm for **5**, and this can be related to the short intramolecular Pt···H contact distance (see above). The infrared data for **5** and **6** at the solid state show intense and sharp bands at 1524 and 1528 cm^{-1}, respectively, attributable to the $CH_2{=}CH_2$ stretching vibration coupled to the CH_2 bending mode, some 100 cm^{-1} lower energy than the band for free ethylene.

Keywords: Tenoxicam; Meloxicam; X-ray diffraction; Dimethylsulfoxide

1. Introduction

Non-steroidal anti-inflammatory drugs (NSAIDs) from the 'oxicam' family (Scheme 1) showed to be strong chelators for several divalent metal ions from the 'block-d' of the periodic table, via the amide oxygen

* Corresponding author. Tel.: +39-0577-234368; fax: +39-0577-234177.
E-mail address: cini@unisi.it (R. Cini).

0277-5387/03/$ - see front matter © 2003 Elsevier Science Ltd. All rights reserved.
doi:10.1016/S0277-5387(03)00112-8

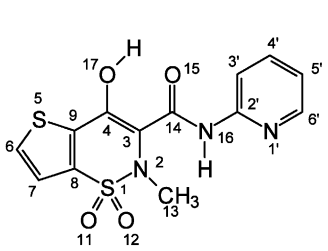

Tenoxicam, H_2ten

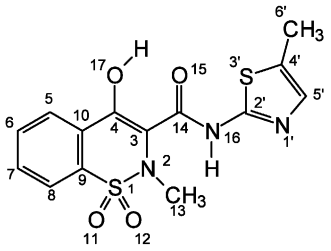

Meloxicam, H_2mel

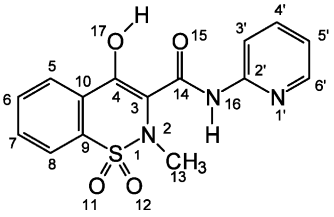

Piroxicam, H_2pir

Scheme 1. Structural formula for tenoxicam (H_2ten), meloxicam (H_2mel) and piroxicam (H_2pir). The numbering of the atoms used in this paper is also reported. The molecules have the 17,1′-EZE conformation.

atom and nitrogen atoms from the pyridyl or thiazolyl rings [1]. In this type of compounds the enol oxygen atom is always deprotonated, is not linked to the metal but instead is linked to the N–H function via a strong intramolecular hydrogen bond made possible by the ZZZ conformation at the C(3)–C(4), C(14)–N(16), and N(16)–C(2′) vectors. When a bis chelate to M(II) is formed through this coordination mode a neutral complex molecule is formed and the arrangement of the two ligand anions is trans, probably to minimize the steric hindrance. The coordination sphere arrangement is pseudo-octahedral with two solvent molecules as apical ligands (at least for dmso and dmf) [1b,1e]. Provided the apical ligands are hydrophobic molecules, the full octahedral complex molecules have a high hydrophobic character on the external surface, which is an important factor to decrease the extent of attack by hydrophilic species in the solution phase and to facilitate transport across membranes (see Refs. [1b,2] and references therein). Therefore, the hydrophobicity of the molecules has to be sought in designing pharmaceutically active coordination compounds [2a,2b].

The involvement of the enolate oxygen atom of 'oxicam' ligands in the coordination to the metals has been clearly shown only in the case of a Sn(IV) complex [1a,1f] and this is related to the high affinity of this metal ion towards the oxygen donor, and to the deprotonated form of the ligand used in the preparative procedure (pir^{2-}, ten^{2-}; H_2pir, piroxicam).

In the case *trans*-$[PtCl_3(\eta^2\text{-}C_2H_4)]^-$ or *trans*-$[PtCl_2(dmso)_2]$ are used as the starting metal containing reactants with H_2pir, *trans*-$[PtCl_2(H_2pir)L]$ type complexes were obtained and the H_2pir molecule adopted the EZE conformation [1c.1d].

With the aim to continue the exploration of the coordination mode adopted by 'oxicam' NSAIDs we have performed a preparative and structural work by using tenoxicam and meloxicam as ligands and some 'block-d' metal ions, and we wish to report here on some results from the investigation.

2. Experimental

2.1. Materials

$Zn(CH_3COO)_2\cdot 2H_2O$ (Erba), $Cd(CH_3COO)_2\cdot 2H_2O$ (Erba), $K[PtCl_3(\eta^2\text{-}C_2H_4)]\cdot H_2O$ (Janssen), 4-hydroxy-2-methyl-*N*-(5-methyl-2-thiazolyle)-2H-1,2-benzothiazine-3-carboxammide-1,1-dioxide (meloxicam, Boehringer Ingelheim), 4-hydroxy-2-methyl-*N*-2-pyrimidyl-2H-thieno[2,3-e]-1,2-thiazine-3-carboxamide-1,1-dioxide (tenoxicam, Sigma-Aldrich) were used as purchased without any further purification. Chloroform ($CHCl_3$, Baker), dimethylsulfoxide (dmso, analytical grade (a.g.) BDH), ethanol 99% (EtOH, a.g., Baker), methanol (MeOH, a.g., Baker), ethyl ether (Et_2O, a.g., Baker) were also used without any further purification. $Fe(CH_3COO)_2\cdot 4H_2O$ was prepared as previously reported [3].

2.2. Synthesis

2.2.1. $M^{II}(Hten)_2 \cdot nL$ (M: Cd, **1**; Co, **2**; Zn, **3**. L: CH_3OH, H_2O)

The complexes were prepared according to the following procedure. Tenoxicam (88 mg, 0.25 mmol) and the respective metal acetate (33 mg, **1**; 31 mg, **2**; 27 mg, **3**; 0.125 mmol) were separately dissolved in hot methanol (40 and 5 ml, respectively). The two clear solutions were mixed and the final mixture was refluxed under stirring for approximately 0.5 h. The complexes precipitated as microcrystalline powders after a few minutes from mixing. The yellow solid compounds were filtered, washed with hot methanol, and then dried under vacuum at room temperature. Yields: 60–88%. $Cd^{II}(Hten)_2 \cdot 2CH_3OH$, **1**. *Anal.* Calc. for $C_{28}H_{28}CdN_6O_{10}S_4$ (MW, 849.25): C, 39.60; H, 3.56; N, 9.90; S, 15.10. Found: C, 39.61; H, 3.34; N, 10.03; S, 15.30. IR (KBr matrix): 1324 cm^{-1} (strong, s; $\nu_{asym}(SO_2)$); 1147 cm^{-1} (medium, m; $\nu_{sym}(SO_2)$). UV in $CHCl_3$: 366 nm (ε, 27 480 $cm^{-1}\,mol^{-1}\,dm^3$).

$Co^{II}(Hten)_2 \cdot CH_3OH \cdot 3H_2O$, **5**. *Anal.* Calc. for $C_{27}H_{30}CoN_6O_{12}S_4$ (MW, 817.77): C, 39.65; H, 3.69; N, 10.28; S, 15.68. Found: C, 39.75; H, 3.55; N, 10.28; S, 15.74. IR (KBr matrix): 1328 cm^{-1} (s; $\nu_{asym}(SO_2)$); 1152 cm^{-1} (m; $\nu_{sym}(SO_2)$). UV in $CHCl_3$: 396 nm (ε, 19 183 $cm^{-1}\,mol^{-1}\,dm^3$).

$Zn^{II}(Hten)_2 \cdot 2CH_3OH$, **3**. Calc. for $C_{28}H_{28}N_6O_{10}S_4Zn$ (MW, 802.23), **3**: C, 41.92; H, 3.52; N, 10.47; S, 15.99. Found: C, 41.32; H, 3.62; N, 10.38; S, 15.74. IR (KBr matrix): 1330 cm^{-1} (s; $\nu_{asym}(SO_2)$; 1152 cm^{-1} (m; $\nu_{sym}(SO_2)$). UV in $CHCl_3$: 383 nm (ε, 36 085 $cm^{-1}\,mol^{-1}\,dm^3$).

2.2.2. trans,trans-$[Cd^{II}(Hten)_2(dmso)_2]$, **4**

The crude product **1** was recrystallized from dmso. Single crystals suitable for X-ray diffraction were obtained on slowly cooling a hot saturated dmso solution of **4** and formed within 2 days from the dissolution. The crystals were filtered off, washed two times with MeOH and then dried in the air atmosphere for 24 h at 25 °C. *Anal.* Calc. for $C_{30}H_{32}CdN_6O_{10}S_6$ (MW, 941.44), **4**: C, 38.27; H, 3.43; N, 8.93; S, 20.44. Found: C, 38.57; H, 3.62; N, 9.01; S, 20.37. IR (KBr matrix): 1337 cm^{-1} (s; $\nu_{asym}(SO_2)$); 1150 cm^{-1} (m; $\nu_{sym}(SO_2)$). UV in $CHCl_3$: 376 nm (ε, 21 747 $cm^{-1}\,mol^{-1}\,dm^3$).

2.2.3. trans-$[PtCl_2(\eta^2\text{-}C_2H_4)(H_2ten)]$, **5**

0.3 mmol (120 mg) of $K[PtCl_3(\eta^2\text{-}C_2H_4)]H_2O$ were dissolved in 20 ml of EtOH at room temperature, whereas 0.3 mmol (101 mg) of tenoxicam were dissolved in 40 ml of EtOH at approximately 60 °C. The two clear solutions were mixed and the temperature quickly lowered to 25 °C. The mixture was stirred at room temperature for 30 min. The complex precipitated as microcrystalline powder after a few minutes from mixing. The solid compound was filtered, washed with EtOH and Et_2O, and then dried under vacuum at room temperature. The crude product was recrystallized from benzene. Yield: 66%. *Anal.* Calc. for $C_{15}H_{15}Cl_2N_3O_4S_2Pt$ (MW, 631.41), **5**: C, 28.53; H, 2.39; N, 6.65; Cl, 11.23. Found: C, 28.58; H, 2.35; N, 6.74; Cl, 11.49. Single crystals suitable for X-ray diffraction studies were obtained on slow cooling and evaporating a hot benzene solution of **5**. IR (KBr matrix): 1352 cm^{-1} (s; $\nu_{asym}(SO_2)$); 1162 cm^{-1} (m; $\nu_{sym}(SO_2)$). UV in $CHCl_3$: 348 nm (ε, 22 231 $cm^{-1}\,mol^{-1}\,dm^3$).

2.2.4. trans-$[PtCl_2(\eta^2\text{-}C_2H_4)(H_2mel)] \cdot 0.25CHCl_3$, **6**·$0.25CHCl_3$ and trans-$[PtCl_2(\eta^2\text{-}C_2H_4)(H_2mel)] \cdot 0.5C_6H_6$, **6**·$0.5C_6H_6$

The preparative procedure was that reported above for **5**. The crude solid obtained from direct reaction of the Zeise's salt and H_2mel in EtOH was recrystallized from $CHCl_3$. *Anal.* Calc. for $C_{16.25}H_{17.25}Cl_{2.75}N_3O_4S_2Pt$ (MW, 675.29), **6**·0.25$CHCl_3$: C, 28.90; H, 2.57; N, 6.22; S, 9.50. Found: C, 29.32; H, 2.52; N, 6.03; S, 9.08. Single crystals suitable for X-ray diffraction studies of **6**·$0.5C_6H_6$ were obtained on slow cooling and evaporating a hot benzene solution of **6**·0.25$CHCl_3$. IR (KBr matrix): 1331 cm^{-1} (s; $\nu_{asym}(SO_2)$); 1180 cm^{-1} (m; $\nu_{sym}(SO_2)$). UV in $CHCl_3$: 344 nm (ε, 20 783 $cm^{-1}\,mol^{-1}\,dm^3$).

2.2.5. $Fe^{II}(Hmel)_2 \cdot 4H_2O$, **7**

Meloxicam (351 mg, 1.0 mmol) and $Fe(CH_3COO)_2 \cdot 4H_2O$ (130 mg, 0.5 mmol) were dissolved separately in deaerated hot MeOH (150 and 20 ml, respectively). The two clear solutions were mixed under a stream of nitrogen. The final solution was refluxed under nitrogen for approximately 0.5 h. A microcrystalline orange powder precipitated after a few minutes. The crystalline solid was filtered and washed with deaerated hot MeOH under nitrogen, then was dried under the vacuum at room temperature. The resulting solid was stable in air for many days. Yield: 88%. Found: C, 40.94; H, 4.25; N, 9.57; S, 14.55. Calc. for $C_{30}H_{40}FeN_6O_{14}S_4$ (MW, 892.78): C, 40.36; H, 4.51; N, 9.41; S, 14.36. IR (KBr matrix): 1330 cm^{-1} (s; $\nu_{asym}(SO_2)$; 1165 cm^{-1} (s; $\nu_{sym}(SO_2)$). UV in $CHCl_3$: 350 nm (ε, 25 605 $cm^{-1}\,mol^{-1}\,dm^3$).

2.3. X-ray crystallography

2.3.1. Data collections

The data collections for all the crystals were performed through a Siemens P4 automatic four circle diffractometer operating at 295 ± 2 K (unless otherwise specified) with a graphite monochromatized Mo–Kα radiation (λ, 0.71073 Å). The intensities were corrected

Table 1
Selected crystal data and structure refinement parameters for *trans,trans*-[$Cd^{II}(Hten)_2(dmso)_2$], **4**, *trans*-[$PtCl_2(\eta^2\text{-}C_2H_4)(H_2ten)$], **5** and *trans*-[$PtCl_2(\eta^2\text{-}C_2H_4)(H_2mel)$]·$0.5C_6H_6$, **6**·$0.5C_6H_6$

Parameter	**4**	**5**	**6**·$0.5C_6H_6$
Empirical formula	$C_{30}H_{32}CdN_6O_{10}S_6$	$C_{15}H_{15}Cl_2N_3O_4PtS_2$	$C_{19}H_{20}Cl_2N_3O_4PtS_2$
Formula weight	941.38	631.41	684.49
Temperature (K)	293(2)	293(2)	293(2)
Wavelength (Å)	0.71073	0.71073	0.71073
Crystal system	monoclinic	monoclinic	triclinic
Space group	$P2_1/n$	$P2_1/c$	$P\bar{1}$
a (Å)	7.823(1)	12.468(1)	7.080(4)
b (Å)	14.215(1)	7.825(1)	10.777(5)
c (Å)	17.261(1)	20.641(1)	15.182(8)
α (°)	90	90	91.19(4)
β (°)	97.62(1)	98.06(1)	90.18(5)
γ (°)	90	90	95.43(4)
Volume ($Å^3$)	1902.5(3)	1993.9(3)	1152.9(10)
Z	2	4	2
Calculated density ($Mg\,m^{-3}$)	1.643	2.103	1.972
Reflections collected (unique)	4374/3292 [$R_{int} = 0.0269$]	7028/3516 [$R_{int} = 0.0395$]	3990 [$R_{int} = 0.0663$]
Refinement method	full-matrix least-squares on F^2	full-matrix least-squares on F^2	full-matrix least-squares on F^2
Final R indices[$I > 2\sigma(I)$]	$R_1 = 0.0389, wR_2 = 0.0968$	$R_1 = 0.0389$, $wR_2 = 0.0950$	$R_1 = 0.0774$, $wR_2 = 0.1700$
R indices (all data)	$R_1 = 0.0492, wR_2 = 0.1029$	$R_1 = 0.0490$, $wR_2 = 0.1015$	$R_1 = 0.1416$, $wR_2 = 0.2063$

for Lorentz-polarization effects, and absorption effects (via the ψ-scan technique based on at least three reflections) by using the XSCANS package [4]. The selected crystallographic data are listed in Table 1.

*2.3.1.1. trans,trans-[$Cd^{II}(Hten)_2(dmso)_2$], **4**.* A well formed yellow parallelepiped with dimensions $0.40 \times 0.35 \times 0.30$ mm was selected through the polarizing microscope and mounted on a glass fiber. The accurate cell constant determination was obtained via the least-squares method applied to the values of 24 randomly selected strong reflections measured via the automatic diffractometer in the range $18 \leqslant 2\theta \leqslant 40°$. The crystal belongs to the monoclinic system.

*2.3.1.2. trans-[$PtCl_2(\eta^2\text{-}C_2H_4)(H_2ten)$], **5**.* A well formed pale yellow parallelepiped ($0.50 \times 0.30 \times 0.25$ mm) was mounted and analyzed by following the procedure above described for **5**. The crystal belongs to the monoclinic system and the accurate cell constants were determined from the values of 30 randomly selected reflections in the range $7 \leqslant 2\theta \leqslant 40°$.

*2.3.1.3. trans-[$PtCl_2(\eta^2\text{-}C_2H_4)(Hmel)_2$]·$0.5C_6H_6$, **6**·$0.5C_6H_6$.* A pale yellow irregularly shaped fragment ($\approx 0.40 \times 0.30 \times 0.20$ mm) was mounted and analyzed through the procedure above described for **5** and **6**. The crystal belong to the triclinic system and the cell constants were obtained from the values of 29 randomly selected reflections in the range $7 \leqslant 2\theta \leqslant 22°$.

2.4. Structure solution and refinement

The structure of **4** was solved through the Patterson and difference-Fourier techniques followed by series of least-squares cycles. The model was refined in the $P2_1/n$ space group. All the hydrogen atoms were located through the HFIX and AFIX options of SHELX-97 [5]. All the not-hydrogen atoms were refined as anisotropic whereas the hydrogen atoms were treated as isotropic. The analysis of the geometrical parameters was performed by using the PARST-97 package [6] whereas the molecular graphics was carried out via the ORTEP-3 [7], and XPMA and ZORTEP-98 [8] packages. All the calculations were carried out through Pentium III machines.

The structure of **5** was solved through the Patterson and difference-Fourier techniques followed by series of least-squares cycles. The model was refined in the $P2_1/c$ space group. The hydrogen atoms H(11E), H(12E), H(21E) and H(22E) were located by difference-Fourier techniques and were included in the subsequent least-squares cycles of refinement by restraining the C–H distances at 1.10(2) Å via the DFIX options of SHELX-97. The other hydrogen atoms were located through the HFIX and AFIX options. All the not-hydrogen atoms were refined as anisotropic whereas the hydrogen atoms were treated as isotropic.

The structure of **6**·$0.5C_6H_6$ was solved via the Patterson and difference-Fourier techniques followed by series of least-squares cycles. The space group is $P\bar{1}$. All the H atoms have been located in calculated positions through the HFIX and AFIX options of SHELX-97. The non-hydrogen atoms were refined as

anisotropic whereas the hydrogen atoms were considered as isotropic.

2.5. Spectroscopy

The IR spectra were recorded (298 K) via KBr pellet technique on a Perkin-Elmer model 1600 Fourier-transform spectrometer. The ^{1}H NMR spectra were obtained (295 K, 0.01 mol dm^{-3}) through Bruker AC-200 and Bruker DRX 600 spectrometers. The UV–Vis spectra (298 K, 5×10^{-5} mol dm^{-3}) were recorded through a Perkin-Elmer EZ-201 spectrophotometer.

3. Results and discussion

3.1. X-ray structure of trans,trans-[Cd^{II}(dmso)$_2$(Hten)$_2$], 4

The structure of **4** is represented in Fig. 1, whereas the selected geometrical parameters are listed in the Tables 2 and 3.

3.1.1. The coordination sphere

The coordination sphere is pseudo-octahedral and the metal ion sits on the inversion center. The Hten$^-$ anions chelate the metal center through the nitrogen atoms from the pyridine moieties (N(1′)) and through the amidic oxygen atoms (O(15)) at the equatorial positions (with a trans arrangement). The apical coordination sites are occupied by the (O(1D)) oxygen atoms of the two dmso ligands. The Cd–N(1′) bond distance is 2.303(3) Å and is slightly longer than the values found for similar complexes such as *trans,trans*-[Cd^{II}(Hpir)$_2$(dmf)$_2$] [1e] (Hpir$^-$, monoanion of piroxicam; dmf, *N*,*N*-dimethylformammide) and *trans,trans*-[Cd^{II}(Hmel)$_2$(dmso)$_2$] [1b] (Hmel$^-$, monoanion of meloxicam); whereas the Cd–O(15) bond length (2.214(2) Å) is shorter than the values found for those complexes.

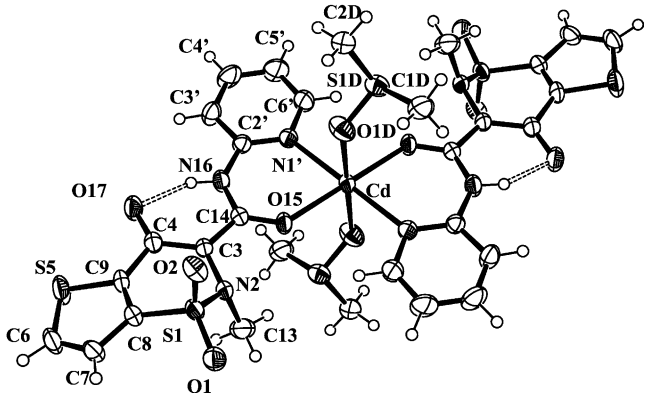

Fig. 1. ORTEP drawing of the complex molecule for *trans,trans*-[Cd^{II}(dmso)$_2$(Hten)$_2$], **4**, with the labeling of the atoms. Ellipsoids enclose 30% probability.

Table 2
Selected bond lengths (Å) for *trans,trans*-[Cd^{II}(Hten)$_2$(dmso)$_2$], **4**

Vector	Distance
Cd(1)–O(15)	2.214(2)
Cd(1)–N(1′)	2.303(3)
Cd(1)–O(1D)	2.310(3)
S(1D)–O(1D)	1.520(3)
S(1)–O(1)	1.429(3)
S(1)–O(2)	1.425(3)
S(1)–N(2)	1.630(3)
S(1)–C(9)	1.743(4)
S(5)–C(8)	1.711(4)
O(15)–C(14)	1.252(4)
O(17)–C(4)	1.264(5)
N(2)–C(3)	1.445(4)
N(2)–C(13)	1.482(5)
N(16)–C(14)	1.366(5)
N(16)–C(2′)	1.391(5)
N(1′)–C(2′)	1.337(5)
C(3)–C(4)	1.407(5)
C(3)–C(14)	1.434(5)

Table 3
Selected bond angles (°) for *trans,trans*-[Cd^{II}(Hten)$_2$(dmso)$_2$], **4**

Vectors	Angle
O(15)–Cd(1)–N(1′)	98.52(10)
O(15)–Cd(1)–O(1D)	89.84(11)
N(1′)–Cd(1)–O(1D)	95.73(12)
O(1D)–S(1D)–C(2D)	104.79(19)
O(1D)–S(1D)–C(1D)	104.4(2)
O(2)–S(1)–O(1)	118.9(2)
O(2)–S(1)–N(2)	108.26(17)
O(1)–S(1)–N(2)	108.40(18)
C(8)–S(5)–C(6)	91.7(2)
C(14)–O(15)–Cd(1)	132.1(2)
C(3)–N(2)–C(13)	114.7(3)
C(3)–N(2)–S(1)	116.0(2)
C(13)–N(2)–S(1)	116.7(3)
C(14)–N(16)–C(2′)	133.0(3)
C(2′)–N(1′)–C(6′)	117.2(3)
C(2′)–N(1′)–Cd(1)	127.8(2)
C(4)–C(3)–C(14)	124.0(3)
C(4)–C(3)–N(2)	121.1(3)
C(14)–C(3)–N(2)	114.7(3)
O(17)–C(4)–C(3)	125.3(3)
C(3)–C(4)–C(8)	115.9(3)
O(15)–C(14)–N(16)	123.9(3)
O(15)–C(14)–C(3)	120.6(3)
N(16)–C(14)–C(3)	115.5(3)

3.1.2. The Hten$^-$ ligand

The tenoxicam ligand is deprotonated at O(17) and is in the 17,1′-ZZZ conformation (see above, Scheme 1). The chelating ligand is stabilized by a strong intramolecular hydrogen bond which involves the O(17) and the N(16) atoms (O···N, 2.618(3) Å; O···H–N, 143.5(2)°). The O(17)–C(4) and C(4)–C(3) bond distances (1.264(5) and 1.407(5) Å, respectively) are similar to the values

found for *trans,trans*-[$Cd^{II}(Hpir)_2(dmf)_2$] [1f] and *trans,trans*-[$M^{II}(Hmel)_2(dmso)_2$] (M, Co, Cd and Zn) [1b]. The torsion angles C(14)–C(3)–C(4)–O(17) (−3.8(6)°), C(4)–C(3)–C(14)–N(16) (−2.0(5)°) and C(4)–C(3)–C(14)–O(15) (179.5(3)°) show that the O(17)–C(4)–C(3)–C(14)((O15))–N(16) segment is almost planar.

The S(1)–O(1) and S(1)–O(2) bond distances are 1.429(3) and 1.425(3) Å, respectively and are close to the distances found for *trans,trans*-[$Cd^{II}(Hpir)_2(dmf)_2$] [1e] and *trans,trans*-[$M^{II}(Hmel)_2(dmso)_2$] (M, Co, Cd and Zn) [1b]. The S(1)–N(2) bond distance is 1.630(3) and is in agreement with those found for other C–SO_2–NH–C groups [9]. The analysis of the puckering on the basis of Cremer and Pople [10] theory for the thiazine ring gives an envelope conformation (with $\theta = 117.02(2)°$, $\phi = -156.59(2)°$ and $Q_T = 0.5139(1)$ Å) which facilitates the formation of a weak intramolecular H-bond between O(1) and H–C(13) (O···C 2.831(6) Å; O···H 2.39(1) Å; O···H–C 108(1)°).

3.1.3. The dmso ligand

The dmso ligand has two possible donor sites, O(1D) and S(1D); the first one being used for **4**. This can be explained on the basis of the steric hindrance. In fact, a coordination of two dmso ligands through S(1D) even at the apical positions should bring to a more crowded complex molecule when compared to **4**. The S(1D)–O(1D) bond distance is 1.520(3) Å and it is similar to those found for [$M^{II}(Hmel)_2(dmso)_2$] (M, Co, Cd and Zn) [1b]. The O(1D)–S(1D)–C(D) bond angles are 104.4(2) and 104.79(19)°.

3.1.4. Crystal packing

There are not interactions between the metal center and the S atom of the thieno system and between the metal center and the SO_2 system, whereas there are weak intermolecular H-bond type interactions between S(5) and H(1D2)–C(1D) ($x-1/2$, $y+1/2$, $z-1/2$) (S···C 3.430(3) Å, S···H 2.96(1) Å; S···H–C 118(1)°), O(1) and H(3′)–C(3′) ($-x+1/2$, $y+1/2$, $-z+1/2+1$) (O···C 3.324(6) Å, O···H 2.71(1) Å; O···H–C 124(1)°) and between O(1) and H(13)–C(13) ($-x$, $-y+1$, $-z+1$) (O···C 3.654(6) Å, O···H 2.82(1) Å; O···H–C 146(1)°). Significant intermolecular stacking interactions do not exist and the molecule shows an overall hydrophobic character on the exterior surface.

3.2. X-ray structure of trans-[$PtCl_2(\eta^2$-$C_2H_4)(H_2ten)$], 5

The molecular structure is represented in Fig. 2 and the geometrical parameters are listed in Tables 4 and 5.

3.2.1. The coordination sphere

The coordination sphere is square planar and the metal is bonded to two chlorine atoms (trans each other), to the N(1′) nitrogen atom from the pyridine moieties and to the ethylene molecule. The Pt(1)–Cl distances average 2.267(2) and are smaller than the corresponding values found for similar structures (*trans*-[$PtCl_2(\eta^2$-$C_2H_4)(H_2pir)$] [1c] (2.297(3) and 2.293(3) Å),

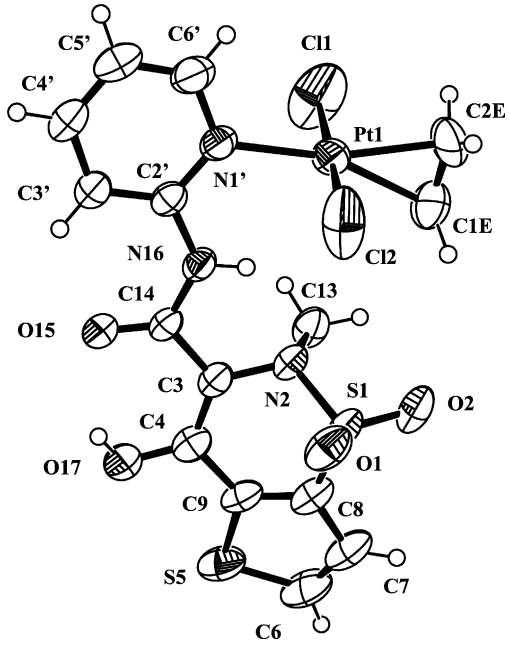

Fig. 2. ORTEP drawing of the complex molecule for *trans*-[$PtCl_2(\eta^2$-$C_2H_4)(H_2ten)$], **5**, with the labeling of the atoms. Ellipsoids enclose 30% probability.

Table 4
Selected bond lengths (Å) for *trans*–[$PtCl_2(\eta^2$–$C_2H_4)(H_2ten)$], **5**

Vector	Distance
Pt(1)–Cl(1)	2.268(3)
Pt(1)–Cl(2)	2.266(2)
Pt(1)–N(1′)	2.077(5)
Pt(1)–C(1E)	2.144(7)
Pt(1)–C(2E)	2.160(8)
S(1)–O(1)	1.419(5)
S(1)–O(2)	1.423(5)
S(1)–N(2)	1.652(5)
S(1)–C(8)	1.748(8)
S(5)–C(6)	1.711(9)
S(5)–C(9)	1.710(7)
N(1′)–C(2′)	1.353(8)
N(1′)–C(6′)	1.356(8)
N(2)–C(3)	1.437(8)
N(2)–C(13)	1.486(8)
N(16)–C(14)	1.368(8)
N(16)–C(2′)	1.381(7)
O(15)–C(14)	1.226(7)
O(17)–C(4)	1.340(8)
C(3)–C(4)	1.363(9)
C(3)–C(14)	1.452(8)
C(4)–C(9)	1.449(8)
C(1E)–C(2E)	1.350(13)

Table 5
Selected bond angles (°) for *trans*–[$PtCl_2(\eta^2–C_2H_4)(H_2ten)$] (**5**)

Vectors	Angle
Cl(2)–Pt(1)–Cl(1)	178.86(11)
N(1′)–Pt(1)–Cl(1)	89.22(17)
C(1E)–Pt(1)–Cl(1)	91.7(3)
C(2E)–Pt(1)–Cl(1)	91.8(3)
N(1′)–Pt(1)–Cl(2)	89.78(16)
C(1E)–Pt(1)–Cl(2)	89.0(3)
C(2E)–Pt(1)–Cl(2)	89.3(3)
N(1′)–Pt(1)–C(1E)	160.0(3)
N(1′)–Pt(1)–C(2E)	163.4(3)
C(1E)–Pt(1)–C(2E)	36.6(4)
O(1)–S(1)–O(2)	120.0(3)
O(1)–S(1)–N(2)	108.1(3)
O(2)–S(1)–N(2)	107.6(3)
O(1)–S(1)–C(8)	109.0(4)
O(2)–S(1)–C(8)	110.2(4)
N(2)–S(1)–C(8)	100.0(3)
C(9)–S(5)–C(6)	90.7(4)
C(2′)–N(1′)–C(6′)	118.0(5)
C(3)–N(2)–C(13)	113.8(5)
C(3)–N(2)–S(1)	113.6(4)
C(13)–N(2)–S(1)	115.3(4)
C(14)–N(16)–C(2′)	129.7(5)
N(1′)–C(2′)–N(16)	114.6(5)
N(16)–C(2′)–C(3′)	123.1(6)
C(4)–C(3)–N(2)	120.8(5)
C(4)–C(3)–C(14)	121.6(6)
N(2)–C(3)–C(14)	117.5(5)
O(17)–C(4)–C(3)	123.9(6)
O(17)–C(4)–C(9)	116.2(6)
C(3)–C(4)–C(9)	119.9(6)
O(15)–C(14)–N(16)	124.0(5)
O(15)–C(14)–C(3)	122.1(6)
N(16)–C(14)–C(3)	113.9(5)
C(2E)–C(1E)–Pt(1)	72.4(5)
C(1E)–C(2E)–Pt(1)	71.1(5)

trans-[$PtCl_2(\eta^2$-$C_2H_4)$(ACV)] [11] (2.302(1) and 2.291(1) Å) (ACV, acyclovir) and *trans*-[$PtCl_2$(dmso)(H_2pir)] [1d]) (2.303(4) and 2.288(4) Å). The Pt(1)–C(1E) and Pt(1)–C(2E) distances are 2.144(7) and 2.160(8) Å in agreement with those found for *trans*-[$PtCl_2(\eta^2$-$C_2H_4)(H_2$pir)] [1c] (2.150(5) and 2.143(6) Å), *trans*-[$PtCl_2$(dmso)(H_2pir)] [1d] (2.179(11) and 2.148(10) Å) and [$PtCl_3(\eta^2$-$C_2H_4)]^-$ [12] (2.128(3) and 2.135(3) Å). The Pt(1)–N(1′) bond (2.077(5) Å) is shorter than that found for *trans*-[$PtCl_2(\eta^2$-$C_2H_4)(H_2$pir)] [1c] (2.093(6) Å). The metal deviates 0.0200(3) Å from the plane defined by the two chloride and the nitrogen donors and the middle point of C–C bond of the ethylene (C(1M)), outwards the H(16) atom.

3.2.2. The ethylene ligand

The C(1E)–C(2E) bond distance measures 1.350(13) Å and is shorter than the value found for *trans*-[$PtCl_2(\eta^2$-$C_2H_4)(H_2$pir)] [1c] (1.42(1) Å). The corresponding bond distances for *trans*-[$PtCl_2(\eta^2$-C_2H_4)(ACV)] [11], *trans*-[$PtCl_3(\eta^2$-$C_2H_4)]^-$ [12] and [$PtCl(\eta^2$-$C_2H_4)(Me_2NCH_2CH_2NMe_2)]^+$ [13] are 1.353(8), 1.375(4) and 1.376(3) Å, respectively. The C–C ethylene bond is perpendicular to the coordination plane and the angle between the normal to the plane and the C(1E)–C(2E) vector is 1.5(3)°.

3.2.3. Tenoxicam ligand

The ligand is neutral and shows a 17,1′-EZE conformation with a strong intramolecular hydrogen bond between the O(17)–H group and the O(15)atom (O–H···O, 2.63(1) Å; H···O, 2.00(1) Å; O–H···O, 134(1)°). Other possible weak intramolecular hydrogen bonds involve O(15) and C(3′) (O···H 2.34(1) Å, O···C 2.904(6) Å, O···H–C 119(1)°), and N(2) and N(16) (N···H 2.22(1) Å, N···N 2.680(6) Å, N···H–N 113(1)°).

The C(3)–C(4) (1.363(9)) and C(4)–O(17) (1.340(8) Å) bond distances are different from those found for **4**. These data are explained by different protonation status and conformation of the ligand. The thiazine ring has an envelope puckering on the basis of the Cremer and Pople parameters [10] $\theta = 117.8(7)°$, $\phi = 153.4(8)°$ and $Q_T = 0.531(5)$ Å. This shows that the conformation is not significantly sensitive to the coordination mode (O(15)/N(1′) chelate or N(1′) monodentate) or to the protonation status (O(17) deprotonated or neutral) of tenoxicam. A Cl–Pt(1)–N(1′)–C(2′) torsion angle is −72.9(3)° showing that the pyridine plane is significantly canted with respect to the coordination square (see below).

The H(16) atom deviates by 2.09(1) Å from the coordination plane and is 2.54(1) Å away from the platinum atom (N(16)–H···Pt, 124(1)°), whereas the N(16)···Cl(2) and H(16)···Cl(2) contact distances are 3.451(5) and 2.86(1)Å (N(16)–H···Cl(2), 127(1)°) (Table 6 and Fig. 3). These values suggest that an attractive interaction may exist between the platinum atom and the amidic H(16) atom, and the H(16) and Cl(2) atoms for **5**, even though the latter interaction is the weakest. The existence of an Pt···H–N interaction has been found in other compounds [1c,1d] from this class and is considered important in general because can influence the stability and reactivity of the metal complexes [14] and has been the subject of molecular mechanics investigations [1g]. Selected intramolecular contact distances and angles relevant to N–H···Cl, N–H···Pt systems are reported in Table 6 for comparative purposes.

3.2.4. Crystal packing

The SO_2 system forms weak intermolecular hydrogen bonds with H–C(7) ($-x+1$, $y+1/2$, $-z+1/2$) (O(1)···H–C, 3.53(3) Å; O(1)···H, 2.85(3) Å; O(1)···H–C, 131(1)°), with H–C(6) ($-x+1$, $y+1/2$, $-z+1/2$) (O(2)···H–C, 3.25(3) Å; O(2)···H, 2.35(3) Å; O(2)···H–C, 164(1)°) and with H–C(1E) ($-x+1$, $-y$, $-z+1$) (O(2)

Table 6
Selected contact distances (Å) and angles (°) found for **5**, **6** and analogous molecules

Vectors	**5**	**6**	*trans*-[$PtCl_2(\eta^2\text{-}C_2H_4)(H_2pir)$] [a]	*trans*-[$PtCl_2(dmso)(H_2pir)$] [b]
Pt···H(16)	2.54(1)	2.93(1)	2.70(8)	2.35(1) [c]
Pt···N(16)	3.107(3)	3.32(1)	3.130(8)	3.08(1) [c]
Pt···H(16)–N(16)	124(1)	109(2)	118(2)	110(2)
Cl···H(16)	2.86(1)	2.52(2)	2.72(8)	3.00(1)
Cl···N(16)	3.451(5)	3.25(1)	3.35(1)	3.61(1)
Cl···H(16)–N(16)	127(1)	144.1(9)	144(8)	110(2)

The H(16) atom was located in calculated positrons for all the structures except for *trans*-[$PtCl_2(\eta^2\text{-}C_2H_4)(H_2pir)$] for which it was located via the difference-Fourier synthesis.

[a] See Ref. [1c].

[b] See Ref. [1d].

[c] Mean values.

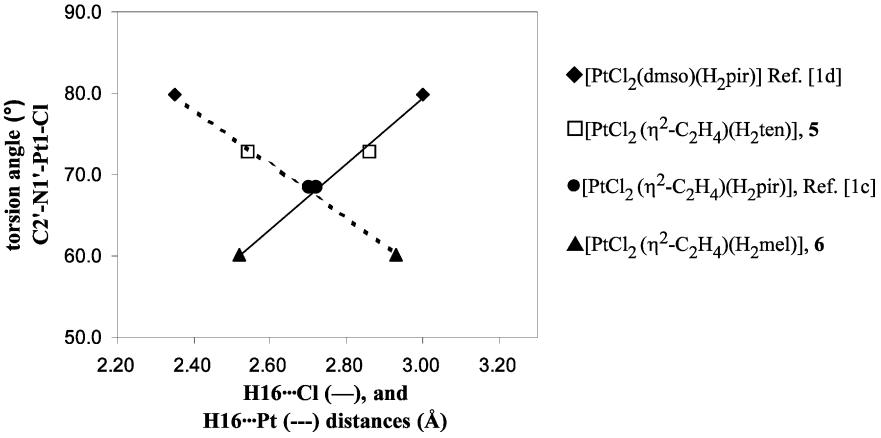

Fig. 3. The picture shows the trend of the H(16)···Cl (—) and H(16)···Pt (---) distances (Å) as a function of the C(2′)–N(1′)–Pt–Cl torsion angle (°), for [$PtCl_2(H_2ox)(L)$] type complexes (H_2ox, generic 'oxicam' ligand).

···H–C, 3.26(3) Å; O(2)···H, 2.37(3) Å; O(2)···H–C, 138(1)°). Stacking type interactions between π-systems from the O(17)C(4)C(3)C(14)(O(15))N(16)C(2′)C(3′) chains are observed for **5** with short C(14)···O(15) contact distances (3.23(5) Å; Fig. 4).

3.3. X-ray structure of *trans*-[$PtCl_2(\eta^2\text{-}C_2H_4)(H_2mel)$]·0.5$C_6H_6$, **6**·0.5$C_6H_6$

The structure **6** is similar to that for **5** for both the coordination mode and conformation of 'oxicam' ligand (Fig. 5). The coordination sphere is square planar and the metal ion is linked to the two chlorine atoms (trans each other), to the N(1′) nitrogen atom from the thiazole moiety and to the ethylene molecule. The Pt(1)–Cl(1) and Pt(1)–Cl(2) distances average 2.300(6) Å (Table 7; the selected angles are listed in Table 8), and are longer than those found for **5**.

The Pt(1)–C(1E) and Pt(1)–C(2E) bond distances are 2.137(18) and 2.134(17) Å, respectively, whereas the N(1′)–Pt(1) bond distance is 2.072(13) Å. These distances are equal to those found for **5** within three times the value of the S.D.

3.3.1. Ethylene ligand

The C(1E)–C(2E) bond distance is 1.37(3) Å and is in agreement with the values found for the **5** (see above). The angle between the C(1E)–C(2E) vector and the normal to the coordination plane is 4(1)°.

3.3.2. Meloxicam ligand

The ligand is neutral and shows the usual EZE conformation, which is stabilized by the strong intra-

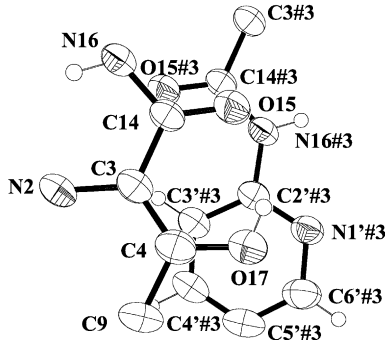

Fig. 4. The diagram shows the overlapping of the O(17)C(4)C(3)C(14)(O(15))N(16)C(2′)C(3′) chains for **5** as revealed at the solid state. The symmetry operation is: #3, $-x$, $-y$, $-z$. The shortest contact distance is C(14)···O(15)#3, 3.23(5) Å. The view is almost perpendicular to the plane defined by O(15) C(14) C(3).

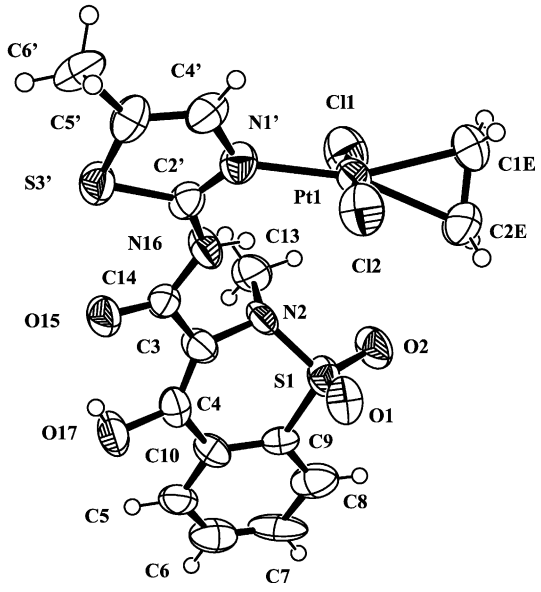

Fig. 5. ORTEP drawing of the complex molecule for *trans*-[$PtCl_2(\eta^2$-$C_2H_4)(H_2mel)]\cdot 0.5C_6H_6$, $\mathbf{6}\cdot 0.5C_6H_6$, with the labeling of the atoms. Ellipsoids enclose 30% probability.

Table 7
Selected bond lengths (Å) for *trans*-[$PtCl_2(\eta^2$-$C_2H_4)(H_2mel)]\cdot 0.5C_6H_6$, $\mathbf{6}\cdot 0.5C_6H_6$

Vector	Distance
Pt(1)–Cl(1)	2.303(6)
Pt(1)–Cl(2)	2.298(6)
Pt(1)–N(1′)	2.072(13)
Pt(1)–C(1E)	2.137(18)
Pt(1)–C(2E)	2.134(17)
S(1)–O(1)	1.406(15)
S(1)–O(2)	1.446(12)
S(1)–N(2)	1.651(15)
S(1)–C(9)	1.753(16)
S(3′)–C(2′)	1.699(15)
S(3′)–C(4′)	1.71(2)
O(15)–C(14)	1.226(18)
O(17)–C(4)	1.359(19)
N(2)–C(3)	1.44(2)
N(2)–C(13)	1.46(3)
N(16)–C(14)	1.35(2)
N(16)–C(2′)	1.40(2)
N(1′)–C(2′)	1.31(2)
N(1′)–C(5′)	1.43(2)
C(3)–C(4)	1.33(2)
C(3)–C(14)	1.49(2)
C(4)–C(10)	1.48(2)
C(1E)–C(2E)	1.37(3)

molecular hydrogen bond between the O(17)H function and the O(15) amidic atom (O···H 1.91(1) Å, O···O 2.62(2) Å, O···H–O 145.1(9)°). The O(17)–C(4)–C(3)–C(14) (O(15))–N(16)–C(2′) segment is almost planar. The maximum deviation is relevant to the C(4)–C(3)–C(14)–N(16) grouping whose torsion angle is −163(2)°. The phenyl and the thiazolyl rings are planar, whereas

Table 8
Selected bond angle (°) for *trans*-[$PtCl_2(\eta^2$-$C_2H_4)(H_2mel)]\cdot 0.5C_6H_6$, $\mathbf{6}\cdot 0.5C_6H_6$

Vectors	Angle
Cl(2)–Pt(1)–Cl(1)	177.4(2)
N(1′)–Pt(1)–Cl(1)	87.7(4)
N(1′)–Pt(1)–Cl(2)	92.6(4)
N(1′)–Pt(1)–C(1E)	158.5(7)
N(1′)–Pt(1)–C(2E)	163.7(7)
C(1E)–Pt(1)–Cl(1)	91.4(7)
C(1E)–Pt(1)–Cl(2)	89.3(7)
C(2E)–Pt(1)–Cl(1)	88.7(7)
C(2E)–Pt(1)–Cl(2)	90.3(7)
C(2E)–Pt(1)–C(1E)	37.5(8)
O(1)–S(1)–O(2)	119.0(8)
O(1)–S(1)–N(2)	108.6(8)
O(2)–S(1)–N(2)	107.8(9)
O(1)–S(1)–C(9)	109.4(9)
O(2)–S(1)–C(9)	109.1(8)
N(2)–S(1)–C(9)	101.5(7)
C(2′)–S(3′)–C(4′)	88.7(8)
C(3)–N(2)–C(13)	115.7(14)
C(3)–N(2)–S(1)	112.7(12)
C(13)–N(2)–S(1)	117.0(11)
C(14)–N(16)–C(2′)	125.4(13)
C(2′)–N(1′)–C(5′)	111.4(13)
C(4)–C(3)–N(2)	121.2(14)
C(4)–C(3)–C(14)	122.5(15)
N(2)–C(3)–C(14)	116.3(14)
C(3)–C(4)–O(17)	122.3(16)
C(3)–C(4)–C(10)	122.5(14)
O(17)–C(4)–C(10)	115.2(15)
O(15)–C(14)–N(16)	123.1(14)
O(15)–C(14)–C(3)	121.6(15)
N(16)–C(14)–C(3)	114.7(13)
N(1′)–C(2′)–N(16)	120.6(13)
C(2E)–C(1E)–Pt(1)	71.1(11)
C(1E)–C(2E)–Pt(1)	71.3(10)

the thiazine ring shows an envelope conformation with $\theta = 65(2)^\circ$, $\phi = 31(2)^\circ$ and $Q_T = 0.53(1)$ Å.

The angle formed between the thiazolyl plane and the coordination plane is of 56.1(4)° and the Cl(2)–Pt(1)–N(1′)–C(2′) torsion angle is −60(1)°. This facilitate the formation of interaction between the H(16) and Cl(2) atoms (H(16)···Cl(2) and N(16)···Cl(2) contact distances, 2.52(2) and 3.25(1) Å; Cl(2)···H–N(16) angle, 144.1(9)°, see Table 6). The Pt(1)···H(16) contact distance is 2.93(1) Å.

3.3.3. Crystal packing

In this structure there are not significant stacking interactions. Weak intermolecular hydrogen bonds between the SO_2 system and thiazolyl H(6′) atom (x, $y+1$, $+z$) (O(2)···H–C, 3.32(3) Å; O(2)···H, 2.42(1) Å; O(2)···H–C, 157(1)°), and enolic H(17) atom ($-x+1$, $-y+1$, $-z+1$) (O(1)···H–O, 3.09(2) Å; O(1)···H, 2.55(1) Å; O(1)···H–O, 124(1)°) stabilize the crystal.

Table 9
Selected infrared absorption bands (cm^{-1}) for **1**, **2**, **3**, **4**, **5**, **6**, **7**, H_2ten and H_2mel

Stretching motion	**1**	**2**	**3**	**4**	**5**	H_2ten	**6**	H_2mel	**7**
NH(amide)					3244		3213	3288	
C=O(amide)	1651	1634	1619	1623	1653	1635	1653	1619	1582
SO_2 asym.	1324	1328	1330	1337	1352	1328	1331	1346	1330
SO_2 sym.	1147	1152	1152	1150	1162	1144	1180	1183	1165
CH_2=CH_2					1524		1528		

3.4. Spectroscopy

3.4.1. Infrared

The selected absorption data are reported in Table 9. No significant absorption band attributable to the N–H stretching vibration could be revealed for the spectra of **1**, **2**, **3**, **4** and **7** in agreement with the presence of a strong intramolecular hydrogen bond between H–N(16) group and O(16) atom for Hten$^-$ and Hmel$^-$ ligands in the 17,1′-ZZZ conformation. The SO_2-vibrations are almost unchanged with respect to free ligands. The absorption band relevant to the stretching motion for the amidic C=O group is in the range 1651–1582 cm^{-1} for **1**, **2**, **3**, **4** and **7**, whereas is at 1635 and 1619 cm^{-1} for the free H_2ten and H_2mel ligand, respectively.

Interestingly the N–H stretching vibration has maxima at 3244 and 3213 $cm^{-1}$for **5** and for **6** with a clear red-shift of 75 cm^{-1} for **6**. A red-shift effect previously found for *trans*-[$PtCl_2(\eta^2$-$C_2H_4)(H_2pir)$] [1c] and *trans*-[$PtCl_2$(dmso)(H_2pir)] [1d] was interpreted on the basis of a M···H–N interaction. The spectrum of free H_2ten has not any sharp band in the region 3400–3200 cm^{-1}, even though a rather broad band centered at 3089 cm^{-1} is mostly attributable to the aromatic C–H vibrations. There is an intense band relevant to the stretching of the C=C bond of ethylene coupled with a bending motion at 1524 cm^{-1} for complex **5** and at 1528 cm^{-1} for complex **6**. The corresponding band for *trans*-[$PtCl_3(\eta^2$-$C_2H_4)]^-$ is reported at 1526 cm^{-1}, some 100 cm^{-1} lower energy than for free ethylene [15].

3.4.2. ^1H NMR

The chemical shifts for the signals of **1** (dmso-d_6, 295 K) are usually shifted towards higher field upon deprotonation of O(17) and complex formation (Table 10). Significant shifts are 0.29 ppm for H(5′) and 0.12 ppm for H(7).

The signals for **5** ($CDCl_3$, 298 K) are shifted towards lower field with respect to free H_2ten. The magnitude of the shift is large for the pyridyl protons in agreement with the metal coordination at N(1′), and for amidic H(16) proton (1.93 ppm). This effect must be related the short intramolecular Pt···H contact distance (see above). The signal of enolic H(17) atom only is upfield shifted (by 0.60 ppm). The signals relevant to the ethylene protons are at 5.11 ppm.

Similarly, the signal for **6** are shifted towards lower fields with a large effect for amidic H(16) proton by some 1.26 ppm. The shift for **6** is therefore smaller than for **5** and this can be related to the larger H(16)···Pt distance for **6** than for **5**. The signal for the enolic H(17)

Table 10
Selected chemical shifts δ, (ppm from tetramethylsilane) in the ^{1}H NMR spectra of **1**, **5** and **6** and free tenoxicam and meloxicam (0.01 mol dm^{-3})

	δ					
Proton	**1** (dmso-d_6)	H_2ten (dmso-d_6)	**5** ($CDCl_3$)	H_2ten ($CDCl_3$)	**6** ($CDCl_3$)	H_2mel ($CDCl_3$)
H[O(17)]			12.56(s)	13.16(s)	12.37(s)	12.72(s)
H[N(16)]	13.25(s)	13.56(s)	10.74(s)	8.81(s)	11.46(s)	10.2(s)
H(6′)	8.19(d)	8.29(d)	8.57(d)	8.40(d)		
H(3′)	≈7.8	7.71(d)	8.39(d)	8.24(d)		
H(4′)	7.72	8.09(t)	7.95(t)	7.78(t)		
H(5)					8.10(d)	8.07(d)
H(8)					7.97(d)	7.91(d)
H(6)	7.80	7.98(d)	7.78(d)	7.74(d)	7.81(m)	7.76(m)
H(7)	7.28(d)	7.40(d)	7.50(d)	7.46(d)	7.81(m)	7.76(m)
H(5′)	6.97(t)	7.26(t)	7.31(t)	7.15(t)	7.48(s)	7.24(s)
H(ethylene)			5.11(s)		4.99(s)	
H(CH_3N)	3.39(s)	3.48(s)	3.11(s)	3.04(s)	3.00(s)	2.85(s)
H6′(CH_3–thiazolyl)					2.48(s)	2.44(s)

proton is upfield shifted by 0.35 ppm. The signals for H (ethylene) protons are at 4.99 ppm for both **5** and **6**.

4. Conclusion

In conclusion this work produced several new crystalline compounds with meloxicam and tenoxicam as ligands. The two molecules show the usual coordination behavior previously found for piroxicam when reacted with divalent metal acetates or with the Zeise's salt in alcoholic media. The amide oxygen and the sp^2-nitrogen from pyridyl or thiazolyl rings chelate the metal ion whereas the enol oxygen atom undergoes deprotonation in the case the weak base acetate is present (the overall conformation of the ligand changes from EZE to ZZZ). Moreover, meloxicam and tenoxicam behave similarly to piroxicam as regard as the reaction with the Zeise's salt, too, the sp^2-nitrogen atom alone being the donor to platinum and the overall ligand conformation being EZE.

It is interesting to note that the ligand conformations around the bonds C(4)–C(3)–C(14)–N(16)–C(2′)–N(1′) do not change much within each class of complexes, $[M(Hox)_2(L)_2]$ and $[PtCl_2(H_2ox)(L')]$. As regards the latter type of compounds, the orientation of the H_2ox ligand with respect to the coordination plane as measured by the Cl–Pt–N(1′)–C(2′) torsion angle changes in the range 60–80°, and it is modulated by several effects, which include intermolecular forces, intramolecular attractions such as H(16)···Pt, H(16)···Cl, H(16)···N(2) and intramolecular clashes.

In the case of $[PtCl_2(H_2mel)(C_2H_4)]$ the H(16)···Cl linking interaction seems to prevail on the H(16)···Pt one (Fig. 3, Table 6) at least at the solid state. It has to be recalled that the red-shift on the infrared absorption band for the N–H stretching vibration is approximately 75 cm^{-1} for $[PtCl_2(H_2mel)(C_2H_4)]$ (H(16)···Pt, 2.93 Å) and approximately 90 cm^{-1} for $[PtCl_2(H_2pir)(C_2H_4)]$ (2.70 Å).

The effect of the metal coordination on the ^1H NMR signal for H(16) of $[PtCl_2(H_2mel)(C_2H_4)]$ is 1.26 ppm, smaller than the corresponding one for $[PtCl_2(H_2pir)(C_2H_4)]$ (1.98 ppm) suggesting that the H(16)···Pt contact distance is, on average, larger for the H_2mel derivative in solution, too (at room temperature).

Several attempts to grow single crystals suitable for X-ray diffraction analysis for $Fe(Hmel)_2\cdot 4H_2O\cdot 2CH_3OH$, **7**, were unsuccessful. Notwithstanding, the analysis of the infrared data suggests that the $Hmel^-$ anion links the metal cation at least via the amide oxygen; the chelations via enol and amide oxygen atoms or via amide oxygen and sp^2-nitrogen atoms cannot be discriminated with the data available.

Finally, the analysis of the molecular structures of metal complexes with other 'oxicam' ligands should help to shed light on the coordinating ability, the conformational space and the electronic properties of this class of ligands. Further efforts aimed to synthesize new complexes are in progress in this laboratory.

5. Supplementary material

Supplementary material has been deposited with the Cambridge Crystallographic Data Centre, CCDC Nos. 197568, 197569, 197570. Copies of this information may be obtained free of charge from The Director, CCDC, 12 Union Road, Cambridge, CB2 1EZ, UK (Fax: +44-1223-336-033; e-mail: deposit@ccdc.cam.ac.uk or www: http://www.ccdc.cam.ac.uk.

Acknowledgements

The authors thank Mr Francesco Berrettini for the data collection at CIADS (Centro Interdipartimentale di Analisi e Determinazione Strutturali, University of Siena) and University of Siena for funding, Boehringer-Ingelheim Italia (Reggello, Florence) is gratefully acknowledged for generous gifts of meloxicam.

References

[1] (a) S.K. Hadjikakou, M.A. Demertzis, J.R. Miller, D. Kovala-Demertzis, J. Chem. Soc., Dalton Trans. (1999) 663;
(b) S. Defazio, R. Cini, J. Chem. Soc., Dalton Trans. (2002) 1888;
(c) D. Di Leo, F. Berrettini, R. Cini, J. Chem. Soc., Dalton Trans. (1998) 1993;
(d) R. Cini, J. Chem. Soc., Dalton Trans. (1996) 111;
(e) R. Cini, G. Giorgi, A. Cinquantini, C. Rossi, M. Sabat, Inorg. Chem. 29 (1990) 5197;
(f) M.A. Demertzis, S.K. Hadjikakou, D. Kovala-Demertzis, A. Koutsodimou, M. Kubicki, Helvetica Chim. Acta 83 (2000) 2787;
(g) T.W. Hambley, Inorg.Chem. 37 (1998) 3767.
[2] (a) J.A. Platts, D.E. Hibbs, T.W. Hambley, M.D. Hall, J. Med. Chem. 44 (2001) 472;
(b) J.E. Weder, T.W. Hambley, B.J. Kennedy, P.A. Lay, G.J. Foran, A.M. Rich, Inorg. Chem. 40 (2001) 1295;
(c) R. Cini, Comments Inorg. Chem. 22 (2000) 151.
[3] R. Cini, Inorg. Chim. Acta 73 (1983) 147.
[4] XSCANS. X-ray Single Crystal Analysis System, Version 2.1 Siemens Analytical X-ray Instruments Inc., Madison, Wisconsin, USA, 1994.
[5] G.M. Sheldrick, SHELX-97, Program for Crystal Structure Determination, University of Göttingen, Göttingen, Germany, 1997.
[6] M. Nardelli, PARST-97, A System of Computer Routines for Calculating Molecular Parameters from Results of Crystal Structure Analysis, University of Parma, Parma, 1997.
[7] C.K. Johnson, M.N. Burnett, ORTEP-3 for Windows, Oak Ridge National Laboratory. 32-bit Implementation by Farrugia, L.J. University of Glasgow, 1998.
[8] L. Zsolnai, XPMA-ZORTEP-98, University of Heidelberg, Germany, 1998.

[9] H.F. Allen, O. Kennard, D.G. Watson, L. Brammer, A.G. Orpen, R. Taylor, J. Chem. Soc., Perkin Trans 2 (1987) S1.
[10] D. Cremer, J.A. Pople, J. Am. Chem. Soc. 97 (1975) 1354.
[11] L. Cavallo, R. Cini, J. Kobe, L.G. Marzilli, G. Natile, J. Chem. Soc., Dalton Trans. (1991) 1867.
[12] R.A. Love, T.F. Koetzle, G.J.B. Williams, L.C. Andrews, R. Bau, Inorg. Chem. 14 (1975) 2653.
[13] G. Gervasio, S.A. Mason, L. Maresca, G. Natile, Inorg. Chem. 25 (1986) 2207.
[14] L.-Y. Huang, U.R. Aulwurm, F.W. Heinemann, F. Knoch, H. Kisch, Chem. Eur. J. 4 (1998) 1641.
[15] K. Nakamoto, Infrared and Raman Spectra of Inorganic and Coordination Compounds, third ed., Wiley, New York, 1978, p. 384.